21st Australasian Fluid Mechanics Conference
Adelaide, Australia
10-13 December 2018

Estimating the Turbulence Length Scales from Cross-Correlation Measurements in the Atmospheric Surface Layer

M.J. Emes, A. Jafari and M. Arjomandi

Centre for Energy Technology, School of Mechanical Engineering
University of Adelaide, Adelaide, South Australia 5005, Australia

Abstract

Dynamic wind effects on small physical structures have been shown to be dependent on the spatial distribution and three-dimensional structure of highly sheared and elongated eddies embedded in anisotropic turbulence due to the presence of the ground. The turbulence length scales in the lowest 10 m of a low-roughness atmospheric surface layer (ASL) during different stability conditions were analysed from the cross-correlation of velocity measurements obtained from field experiments in the Utah desert. Turbulence length scales of the vertical velocity component are largest in magnitude in the convective ASL from the sporadic bursting of turbulence due to buoyancy forces, whereas the spanwise length scales are similar in magnitude to the longitudinal length scales during stable conditions. During neutral conditions, the longitudinal length scales in the low-roughness ASL were not consistent with semi-empirical models and other field measurements, however the ratios of the lateral and vertical length scales with the longitudinal length scales showed good agreement.

Introduction

Velocity fluctuations of shear-generated turbulence are largest near the ground in the atmospheric surface layer (ASL) of nominal 100 m depth, which can lead to dynamic effects such as galloping and flutter on small physical structures on the ground when the turbulence length scales and characteristic length of the physical structure are the same order of magnitude [17]. Turbulence length scales are a measure of the average sizes of the energy-containing eddies that are widely estimated using two-point cross-correlation analysis. The temporal lag of the fluctuating velocities in respective directions are converted to a separation distance in space using Taylor's hypothesis that the convection velocity is equal to the mean velocity at the corresponding height [7, 26]. The Obukhov length scale of the local shear is smaller than the observational height ($L/z < 1$) below the threshold mean horizontal wind speed $U < 4.5$ m/s at $z = 10$ m in the stable nocturnal ASL [20]. In contrast, the eddy sizes increase ($L/z > 1$) at $U \geq 4.5$ m/s as the ASL approaches neutral conditions such that $|z/L| \leq 0.1$ and the gradient Richardson number RI is close to zero. The turbulence quantities and spatial structure of a shear-generated wall-bounded flow in the near-neutral ASL closely approximate those in a laboratory flat-plate boundary layer, except the energy distribution is shifted to larger frequencies and further away from the wall [8, 14, 16]. Turbulent power spectra observations in the ASL have suggested that only the deviations of mean velocities, turbulence variances and length scales of the vertical component show consistent Obukhov scaling from site to site because of the absence of low-frequency components [18]. In contrast, the large variations in longitudinal turbulence length scales shown by field measurements [2, 5] at different sites and predicted by semi-empirical models, such as ESDU 85020 [3] and ESDU 86010 [4]. This is caused by differences in the upstream terrain because the low-frequency components of the horizontal components of turbulence cannot be consistently scaled from site to site [18]. However, the effect of stability and wind speed on the turbulence length scales, particularly in the lateral and vertical directions, is less understood at heights below 10 m in the ASL. Hence, the objective of this study is to estimate the turbulence length scales from cross-correlation measurements with lateral and vertical separations in the ASL for different stability conditions using field measurement data obtained over a very flat, low-roughness terrain at the Surface Layer Turbulence and Environmental Science Test (SLTEST) facility in Dugway, Utah [8]. Dependence of turbulence length scales of the velocity components on height, gradient Richardson number, mean horizontal velocity and friction velocity are compared with semi-empirical models formulated from field measurements over open country terrains.

Experimental Method

Data Measurements

Measurements of wind velocity were acquired from a field experiment study at the SLTEST facility in the western Utah Great Salt Lake desert [1, 8, 9, 13]. The unique geography of the site enabled measurements to be taken in a very high Reynolds number ABL ($Re_* = \delta u_*/\nu \approx 6{\times}10^5$) that has developed over 100 km of low surface roughness salt flats to the north of the SLTEST facility in Dugway Proving Grounds, Utah [12]. Raw temperature and velocity data were measured simultaneously at the SLTEST site for approximately 6 days from 27 May to 3 June 2005 using nine three-dimensional Campbell Scientific CSAT3 sonic anemometers in a vertical tower array at heights $z =$ (1.42, 2.14, 3.00, 4.26, 6.14, 8.71, 12.52, 17.94 and 25.69) m and a spanwise array of ten CSAT3 anemometers at $z = 2.14$ m separated by equal distances $\Delta y = 3$ m to the west of the vertical tower [25]. Three components of velocity in the streamwise x, spanwise y and vertical z directions and absolute temperature θ were measured at a sampling frequency of 20 Hz [8]. All of the anemometers were oriented for predominantly uniform winds from the nominal north at an azimuth angle $\alpha = 0°$ [1, 25]. It was noted by Wilson [24] that the vertical SLTEST tower was positioned near several large instrument trailers. This caused some flow distortion at heights below 6.14 m in the vertical array, such as a 6% reduction in mean wind speed recorded by the anemometer at $z = 3$ m on the vertical tower compared with the anemometers at the same height in a horizontal array positioned at least 10 m west of the tower [13]. Despite this mean velocity discrepancy, comparisons of spectra at the nine heights in the vertical array by McNaughton *et al.* [13] showed an insignificant effect of the disturbed flow by the downwind obstacles.

Data Pre-Treatment

The raw horizontal velocity components u_s and v_s were corrected for the mean wind direction by

$$u_c = u_s \cos\alpha + v_s \sin\alpha \,, \tag{1}$$

$$v_c = v_s \cos\alpha - u_s \sin\alpha \,. \tag{2}$$

Following the wind direction adjustment, the method introduced by Hutchins *et al.* [8] for de-trending the velocity data was used to remove the long-term weather trends and obtain the turbulent fluctuations of the shear-generated flow associated with the average

length scales of eddies in the lowest third of the atmospheric surface layer [15, 19]. The de-trending process, following the method by Hutchins *et al.* [8], applies a low-pass filter to remove the large-scale synoptic wave due to weather phenomena from the fluctuating velocity signal to obtain the turbulent velocity fluctuations. Hence, turbulence intensities and length scales could be with laboratory data and semi-empirical models, such as ESDU 85020 [3] based on similarity theory during neutral conditions.

Stability Criteria

The influence of stratification on the state of the ASL, following Monin-Obukhov similarity theory, is defined by the stability parameter as the ratio of the height to the Obukhov length scale

$$\frac{z}{L} = \frac{g}{\theta_m}\frac{kz\overline{w'\theta'}}{-u_*^3}\,, \tag{3}$$

where g (m/s^2) is the gravitational acceleration, k is von Karman's constant, u_* (m/s) is the friction velocity calculated as $\left(\overline{u'w'}^2 + \overline{v'w'}^2\right)^{1/4}$ in the current study at the reference height $z = 2.14$ m of the SLTEST vertical tower and spanwise array, $\overline{w'\theta'}$ (m/s K) is the surface heat flux and θ_m (K) is the mean potential temperature. An additional parameter used to assess stability conditions in the ASL is the gradient Richardson number,

$$RI = \frac{g}{\theta_m}\frac{\partial\theta}{\partial z}\left(\frac{\partial U}{\partial z}\right)^{-2}\,. \tag{4}$$

Here the gradients of the local potential temperature θ and mean streamwise velocity U are calculated with respect to height z. The gradient Richardson number is positive, zero, and negative for stable, neutral and unstable (convective) conditions, respectively.

Data Selection

Table 1 shows the selected hours, in local time (LT = UTC – 6 h), of the SLTEST velocity data that satisfy the selection criteria for steady winds at $z = 2.14$ m with mean flow angle $|\alpha| = \tan^{-1}(V/U) \leq 20°$. This range was expected to be within the angular response of the sonic anemometers to ensure that the flow was well-aligned with respect to the anemometers for an accurate estimate of the shear stresses and turbulence length scales. For assessment of neutral stability conditions, SLTEST velocity data were selected using the criterion of Högström [6] that $|z/L| \leq 0.1$ for neutral conditions with friction velocity $u_* \geq 0.2$ m/s and mean streamwise velocity $U \geq 5$ m/s at a 2-m height.

Neutral ($\|z/L\| \leq 0.1$)					
Date (2005)	**Time (LT)**	z/L	RI	U **(m/s)**	u_* **(m/s)**
2 June	0400-0500	-0.01	0.02	8.0	0.25
2 June	0500-0600	-0.01	0.02	9.1	0.36
2 June	0600-0700	-0.002	0.03	8.1	0.31
2 June	0700-0800	-0.008	0.03	7.4	0.29
2 June	0800-0900	0	0.02	5.4	0.2
Convective ($z/L <$ -0.1)					
27 May	1500-1600	-0.26	-0.24	5.2	0.16
27 May	1600-1700	-0.3	-0.32	5.3	0.19
27 May	1700-1800	-0.7	-0.55	4.2	0.16
27 May	1800-1900	-2	-0.76	4.2	0.12
Stable ($z/L >$ 0.1)					
27 May	0700-0800	0.72	0.58	1.5	0.05
27 May	0800-0900	0.13	0.15	2.7	0.08
27 May	0900-1000	0.11	0.15	3.1	0.1

Table 1. Selected hours of velocity data at the reference height $z = 2.14$ m on the vertical SLTEST tower for the analysis of different stability conditions.

It is noted that both the mean streamwise velocity U and the friction velocity u_* are largest during the neutral hours in Table 1. In contrast, the mean streamwise and friction velocities decrease marginally during unstable (convective) day-time hours and decrease significantly during stable night-time hours. Hence, mean velocities of shear-generated turbulence are largest in a neutral ASL.

Calculation of Turbulence Length Scales

Point velocity measurements as a function of time can be transformed to spatially distributed data by Taylor's hypothesis. This assumes that eddies are embedded in a frozen turbulence field convected downstream at the mean wind speed U (m/s) in the streamwise direction $\Delta x = U\Delta t$, and hence do not evolve with time t [11]. The integral length scale of the velocity component $i = (u, v, w)$ at a given height z in the ASL is therefore calculated as [21]

$$L_i^x(z) = T_i^x(z)U(z)\,, \tag{5}$$

where T_i^x (s) is the integral time scale of the fluctuating velocity component i, representing the time taken for the average sizes of the energy-containing eddies to traverse a single point in the longitudinal x direction. For example, the longitudinal integral length scale L_u^x (m) at a given height z can be interpreted as the streamwise spacing between two-dimensional spanwise eddies orientated in the axial direction. The integral time scale with longitudinal separation T_i^x is calculated using equation (6) by the integral of the autocorrelation function $R_i(\tau)$ in equation (8) to its first-zero crossing τ_0, assuming that $R_i(\tau)$ fluctuates close to zero after this point [21]. When the autocorrelation curve decreases rapidly to zero, the peak value of the power spectrum is shifted to higher frequencies. The transfer of kinetic energy by the stretching and distortion of larger eddies to smaller eddies becomes excessively large in the high-frequency region of the spectrum, which leads to dissipation by viscosity at the Kolmogorov length scale [22].

$$T_i^x = \int_0^\infty R_i(\tau)\,d\tau \approx \int_0^{\tau_0} R_i(\tau)\,d\tau\,, \tag{6}$$

$$R_i(\tau) = \frac{\overline{i'(t)i'(t+\tau)}}{\sigma_i^2}\,. \tag{7}$$

Here $i = (u, v, w)$ defines the velocity components in the longitudinal x, lateral y and vertical z directions, respectively. The integral length scales with separation distances $j = (y, z)$ in the lateral and vertical directions, respectively, are calculated using the zero-time-delay cross-correlation $R_{ii}(\Delta j, 0)$ of the velocity component i between two points, as follows:

$$R_{ii}(\Delta j, \tau = 0) = \frac{\overline{i'(j)i'(j+\Delta j)}}{\sigma_i(j)\sigma_i(j+\Delta j)}\,, \tag{8}$$

$$L_i^j = \int_{\Delta j=0}^{\Delta j_{\max}} R_{ii}(\Delta j, 0)\,d\Delta j\,. \tag{9}$$

Figure 1 shows sample autocorrelation and cross-correlation functions of the streamwise velocity component during a sample period from 0400 – 0500 LT on 2 June 2005 for comparison with the correlations from Hutchins *et al.* [8]. The autocorrelation function in Figure 1(a) decreases exponentially with longitudinal separation, assuming Taylor's hypothesis $\Delta x = \tau U$, and approaches zero at larger Δx with increasing height in the ASL. The cross-correlation functions of streamwise velocity also decrease with increasing lateral separation Δy and vertical separation Δz in Figure 1(b) and Figure 1(c), respectively, except R_{uu} does not fall below zero. The integral length scales L_u^x, L_u^y and L_u^z are thus calculated using equation (9) by the integration under the curves in Figure 1.

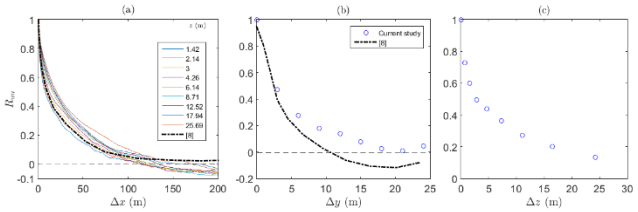

Figure 1. Sample velocity data correlations from 0400 – 0500 LT on 2 June 2005 at $z = 2.14$ m for comparison with Hutchins *et al.* [8]:
(a) Autocorrelation functions R_{uu} of streamwise velocity as a function of longitudinal separation $\Delta x = \tau U$ at different heights in the ASL;
(b) Cross-correlation function R_{uu} of streamwise velocity as a function of lateral separation Δy between anemometers in the spanwise array;
(c) Cross-correlation function R_{uu} of streamwise velocity as a function of vertical separation Δz between anemometers on the SLTEST tower.

Results

Figure 2 presents the turbulence length scales, averaged for each of the three stability conditions in Table 1, with longitudinal separations as a function of height in the SLTEST atmospheric surface layer. Length scales of the streamwise velocity, L_u^x, in Figure 2(a) are proportional to the mean velocity profile $U(z)$, forming a logarithmic profile approaching 30 m during neutral conditions at the maximum measurement height $z = 25.69$ m on the vertical tower. During convective conditions, L_u^x increases to a maximum of 26.8 m at $z = 8.71$ m, but decreases at larger heights. The values of L_u^x during stable conditions are 3-4 times smaller than those during neutral and convective conditions at $z < 10$ m and 2-3 times smaller at $z \geq 10$ m. Length scales of the spanwise velocity, L_v^x, in Figure 2(b) are relatively invariant with height during neutral and convective conditions, but increase linearly with height during stable conditions. Figure 2(c) shows that the length scales of vertical velocity, L_w^x, increase with height for all of the stability conditions. The smallest values of $L_w^x < 5$ m are in the stable nocturnal ASL, whereas L_w^x increases above 5 m at $z \geq 10$ m in the ASL during neutral conditions. The most significant increase in L_w^x above 10 m occurs during daytime hours due to the vertical buoyancy effects from the sporadic bursting of turbulence in the convective (unstable) ASL.

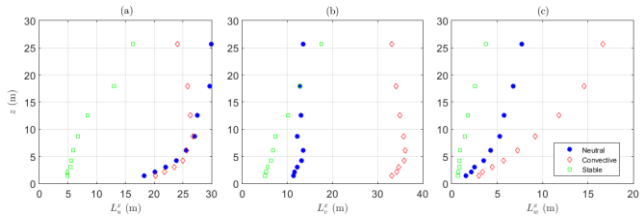

Figure 2. Turbulence length scales, L_i^x, of the (a) streamwise u, (b) spanwise v, and (c) vertical w velocity components, averaged for each of the three different stability conditions in Table 1, as a function of height in the SLTEST atmospheric surface layer.

Figure 3 presents the turbulence length scales, non-dimensionalised with height, during mildly stable conditions as a function of gradient Richardson number calculated using equation (4). Results are compared with equations derived by Kaimal [10] based on stable surface layer measurements for $0.05 \leq RI \leq 0.2$. The non-dimensional streamwise and vertical length scales in Figure 3(a) and Figure 3(c), respectively, show general agreement and convergence with the curves predicted by Kaimal [10]. In contrast, the spanwise length scale L_v^x in Figure 3(c) are significantly larger than those calculated by Kaimal [10]. The results indicate that the spanwise scale of the energy-containing eddies L_v^x/z increases from below 1 in a mildly stable ASL to 2 as the ASL approaches neutral conditions ($RI \rightarrow 0^+$) in the Utah desert.

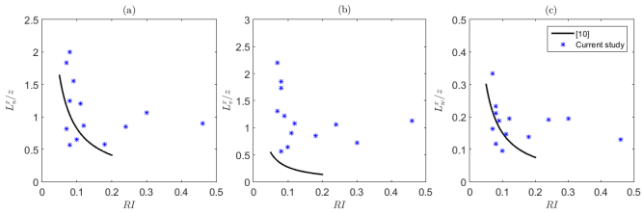

Figure 3. Turbulence length scales, non-dimensionalised with height L_i^x/z, of the (a) streamwise u, (b) spanwise v, and (c) vertical w velocity components with longitudinal separation during mildly stable conditions in Table 1, as a function of gradient Richardson number in the SLTEST atmospheric surface layer. The solid lines show the equations derived by Kaimal [10] based on stable surface layer measurements.

Figure 4(a) shows the variation of the longitudinal length scales with the standard deviation of the fluctuating velocity σ_u at different heights and stability conditions in the SLTEST surface layer. There are defined peaks of $L_u^x = 27$ m at $\sigma_u = 0.5$ m/s in the neutral ASL and $L_u^x = 30$ m at $\sigma_u = 0.6$ m/s in convective conditions, whereas $\sigma_u \leq 0.2$ m/s and is less dependent on σ_u in stable conditions. The non-dimensional length scales L_u^x/z during neutral conditions are strongly correlated to σ_u scaled with U in Figure 4(b) and u_* in Figure 4(c). Hence, the scaling factor of eddy sizes with respect to height is logarithmically proportional to turbulence intensity and friction velocity in a neutral ASL.

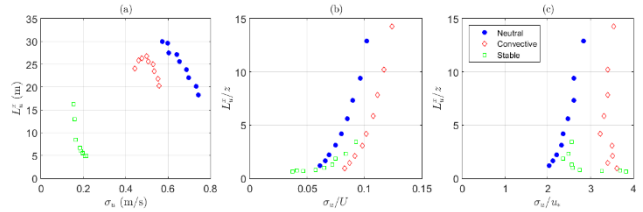

Figure 4. Longitudinal turbulence length scales (a) L_u^x as a function of longitudinal fluctuating velocity standard deviation; (b) non-dimensionalised with height L_u^x/z as a function of longitudinal turbulence intensity σ_u/U; (c) non-dimensionalised with height L_u^x/z as a function of viscous-scaled turbulence intensity σ_u/u_*.

Table 2 shows the longitudinal turbulence length scales calculated by autocorrelation and their ratio with the spanwise and vertical length scales at the standard reference height of 10 m. The average value of L_u^x during neutral hours is 2-3 times smaller than those measured over flat "open country" terrains [5, 23] and an order of magnitude smaller than that predicted by ESDU 85020 [3] during neutral conditions with $U = 8.6$ m/s, $f = 9.5\times10^{-5}$ rad/s and $z_0 = 0.002$ m. The ratios L_v^x/L_u^x and L_w^x/L_u^x in the desert ASL are at least 15% and 35% larger than field measurements by Flay and Stevenson [5] and approximately double those by Teunissen [23]. This suggests that the upstream terrain has a greater effect on L_u^x than on L_w^x, which is in agreement with the findings of Panofsky *et al.* [18]. However, Table 2 shows that the calculated L_u^x in the current study during neutral conditions are not consistent with ESDU 85020 [3] predictions in a low-roughness ASL. This may be due to the small data set limited by the measurement period and the constraints of data selection for steady wind conditions.

Length scales	Current study	ESDU 85020 [3]	Teunissen [23]	Flay and Stevenson [5]
L_u^x (m)	27.2	110	62	88
L_v^x/L_u^x	0.46	0.25	0.18	0.39
L_w^x/L_u^x	0.20	0.09	0.08	0.13

Table 2. Average ratios of turbulence length scales L_i^x of the neutral SLTEST velocity data in Table 1 at the standard reference height $z = 10$ m, compared with ESDU 85020 [3] and field measurements [5, 23].

Table 3 shows the cross-correlation turbulence length scales ratios, compared with those predicted by ESDU 86010 [4] and other field measurements [5, 23]. Overall, there is a good agreement for all of the ratios with those calculated in the current study. This suggests that the scaling of the three-dimensional spatial variation of turbulent energy-containing eddies during neutral conditions in the ASL is consistent and independent of terrain roughness.

Length scales	Current study	ESDU 86010 [4]	Teunissen [23]	Flay and Stevenson [5]
L_u^y/L_u^x	0.28	0.28	0.39	0.24
L_v^y/L_u^x	0.32	0.27	0.46	0.35
L_w^y/L_u^x	0.07	0.05	0.06	0.05
L_u^z/L_u^x	0.27	0.33	–	0.23
L_v^z/L_u^x	0.14	0.16	–	0.26
L_w^z/L_u^x	0.06	0.06	–	0.08

Table 3. Average ratios of turbulence length scales, L_i^y/L_u^x and L_i^z/L_u^x, calculated by cross-correlation of neutral SLTEST velocity data in Table 1 at the reference height $z = 2.14$ m ($L_u^x = 20.1$ m) for the spanwise array and $\bar{z} = 9$ m ($L_u^x = 27.1$ m) for the vertical tower, respectively. Comparison with ESDU 86010 [4] and field measurements [5, 23] at $z =$ 10 m.

Conclusions

Turbulence length scales of the vertical velocity component of the SLTEST data are largest ($L_w^x/z \approx 1$) at $z < 10$ m during convective conditions from buoyancy forces. Neutral longitudinal length scales $L_u^x/z > 1$ at $z \leq 25.69$ m and increase with decreasing height to $L_u^x/z = 12.9$ at $z = 1.42$ m. Length scales of the longitudinal velocity component varied from 18.3 m to 30 m in the height range of the SLTEST vertical tower during neutral conditions, however the average $L_u^x = 27.2$ m at the standard 10-m measurement height was not consistent with semi-empirical models and other field measurements. Average values of L_u^x were up to 4 times smaller at $z = 10$ m than those formulated by ESDU 85020 at $z_0 = 0.002$ m. In contrast, the ratios of the longitudinal and vertical length scales with lateral and vertical separations to the longitudinal length scale, $L_u^y/L_u^x = 0.28$, $L_u^z/L_u^x = 0.32$, $L_w^y/L_u^x = 0.07$ and $L_w^z/L_u^x = 0.06$ showed good agreement with other field measurements. Hence, the scaling effects of the lateral and vertical turbulence components of the three-dimensional turbulence structure in a low-roughness ASL are consistent with similarity theory predictions.

Acknowledgments

Financial support for the work has been provided by the Australian Solar Thermal Research Initiative (ASTRI). The authors acknowledge Associate Professor Nicholas Hutchins, Associate Professor Ivan Marusic, and Dr Kapil Chauhan for their contribution in providing velocity data obtained from the SLTEST facility in Dugway, Utah, USA.

References

[1] Charuchittipan, D. & Wilson, J., Turbulent kinetic energy dissipation in the surface layer, *Boundary-Layer Meteorology*, **132**, 2009, 193-204.
[2] Counihan, J., Adiabatic atmospheric boundary layers: a review and analysis of data from the period 1880–1972, *Atmospheric Environment*, **9**, 1975, 871-905.
[3] ESDU 85020, *Characteristics of atmospheric turbulence near the ground, Part II: single point data for strong winds (neutral atmosphere)*, Engineering Sciences Data Unit, London, UK, 2001.
[4] ESDU 86010, *Characteristics of atmospheric turbulence near the ground, Part III: Variations in space and time for strong winds (neutral atmosphere)*, Engineering Sciences Data Unit, London, UK, 1986.
[5] Flay, R.G.J. & Stevenson, D.C., Integral length scales in strong winds below 20 m, *J Wind Eng Ind Aerodyn*, **28**, 1988, 21-30.
[6] Högström, U.L.F., Non-dimensional wind and temperature profiles in the atmospheric surface layer: A re-evaluation, *Boundary-Layer Meteorology*, **42**, 1988, 55-78.
[7] Hunt, J., Moin, P., Lee, M., Moser, R., Spalart, P., Mansour, N., Kaimal, J. & Gaynor, E., *Cross correlation and length scales in turbulent flows near surfaces*, Springer, 1989, 128-134.
[8] Hutchins, N., Chauhan, K., Marusic, I., Monty, J. & Klewicki, J., Towards reconciling the large-scale structure of turbulent boundary layers in the atmosphere and laboratory, *Boundary-Layer Meteorology*, **145**, 2012, 273-306.
[9] Hutchins, N. & Marusic, I., Evidence of very long meandering features in the logarithmic region of turbulent boundary layers, *Journal of Fluid Mechanics*, **579**, 2007, 1-28.
[10] Kaimal, J., Turbulence spectra, length scales and structure parameters in the stable surface layer, *Boundary-Layer Meteorology*, **4**, 1973, 289-309.
[11] Kaimal, J.C. & Finnigan, J.J., *Atmospheric Boundary Layer Flows: Their Structure and Measurement*, Oxford University Press, 1994.
[12] Marusic, I. & Hutchins, N., Study of the log-layer structure in wall turbulence over a very large range of Reynolds number, *Flow Turbul Combust*, **81**, 2008, 115-130.
[13] McNaughton, K., Clement, R. & Moncrieff, J., Scaling properties of velocity and temperature spectra above the surface friction layer in a convective atmospheric boundary layer, *Nonlin Process Geophys*, **14**, 2007, 257-271.
[14] Metzger, M., McKeon, B.J. & Holmes, H., The near-neutral atmospheric surface layer: turbulence and non-stationarity, *Philos Trans R Soc*, **365**, 2007, 859-876.
[15] Mikkelsen, T., Larsen, S.E., Jørgensen, H.E., Astrup, P. & Larsén, X.G., Scaling of turbulence spectra measured in strong shear flow near the Earth's surface, *Physica Scripta*, **92**, 2017, 124002.
[16] Monty, J., Hutchins, N., Ng, H., Marusic, I. & Chong, M., A comparison of turbulent pipe, channel and boundary layer flows, *Journal of Fluid Mechanics*, **632**, 2009, 431-442.
[17] Nakamura, Y., Bluff-body aerodynamics and turbulence, *J Wind Eng Ind Aerodyn*, **49**, 1993, 65-78.
[18] Panofsky, H.A., Larko, D., Lipschutz, R., Stone, G., Bradley, E., Bowen, A.J. & Højstrup, J., Spectra of velocity components over complex terrain, *Q J R Meteorol Soc*, **108**, 1982, 215-230.
[19] Stull, R.B., *The Atmospheric Boundary Layer*, University of British Columbia, 2005.
[20] Sun, J., Mahrt, L., Banta, R.M. & Pichugina, Y.L., Turbulence regimes and turbulence intermittency in the stable boundary layer during CASES-99, *Journal of the Atmospheric Sciences*, **69**, 2012, 338-351.
[21] Swamy, N.V.C., Gowda, B.H.L. & Lakshminath, V.R., Auto-correlation measurements and integral time scales in three-dimensional turbulent boundary layers, *Applied Scientific Research*, **35**, 1979, 237-249.
[22] Tennekes, H. & Lumley, J.L., *A First Course in Turbulence*, MIT press, 1972.
[23] Teunissen, H.W., Structure of mean winds and turbulence in the planetary boundary layer over rural terrain, *Boundary-Layer Meteorology*, **19**, 1980, 187-221.
[24] Wilson, J., Monin-Obukhov functions for standard deviations of velocity, *Boundary-Layer Meteorology*, **129**, 2008, 353-369.
[25] Wilson, J., Statistics of the Wind-Speed Difference Between Points with Cross-Wind Separation, *Boundary-Layer Meteorology*, **146**, 2013, 149-160.
[26] Yang, H. & Bo, T., Scaling of Wall-Normal Turbulence Intensity and Vertical Eddy Structures in the Atmospheric Surface Layer, *Boundary-Layer Meteorology*, **166**, 2018, 199-216.